ADVANCED FUNCTIONAL MATERIALS
www.afm-journal.de

Materials Views
www.MaterialsViews.com

Bisanthracene-Based Donor–Acceptor-type Light-Emitting Dopants: Highly Efficient Deep-Blue Emission in Organic Light-Emitting Devices

Jian-Yong Hu, Yong-Jin Pu, Fumiya Satoh, So Kawata, Hiroshi Katagiri, Hisahiro Sasabe, and Junji Kido**

Deep-blue fluorescent compounds are particularly important in organic light-emitting devices (OLEDs). A donor–accepotor (DA)-type blue-emitting compound, 1-(10-(4-methoxyphenyl)anthracen-9-yl)-4-(10-(4-cyanophenyl) anthracen-9-yl)benzene (BD3), is synthesized, and for comparison, a nonDA-type compound, 1,4-bis(10-phenylanthracene-9-yl)benzene (BD1) and a weak DA-type compound, 1-(10-phenylanthracen-9-yl)-4-(10-(4-cyanophenyl)anthracen-9-yl)-benzene (BD2), are also synthesized. The twisted conformations of the two anthracene units in the compounds, confirmed by single crystal X-ray analysis, effectively prevent π-conjugation, and the compound shows deep-blue photoluminescence (PL) with a high PL quantum efficiency, almost independent of the solvent polarity, resulting from the absence of an intramolecular charge transfer state. The DA-type molecule BD3 in a non-doped device exhibits a maximum external quantum efficiency (EQE) of 4.2% with a slight roll-off, indicating good charge balance due to the DA-type molecular design. In the doped device with 4,4′-bis(N-carbazolyl)-1,1′-biphenyl (CBP) host, the BD3 exhibits higher EQE than 10% with Commission International de L'Eclairge (CIE) coordinates of (0.15, 0.06) and a narrow full-width at half-maximum of 45 nm, which is close to the CIE of the high definition television standard blue.

1. Introduction

Emitting one of the three primary colors (red, green, and blue), blue fluorescent compounds—besides the corresponding phosphorescent ones—are of interest for applications in organic light-emitting devices (OLEDs). However, because practical long lifetimes are more difficult to achieve for blue-emitting phosphorescent compounds and devices than for blue fluorescent compounds owing to their intrinsic wide energy gap, the latter are of particular importance.[1] It is very challenging to develop efficient and stable deep-blue emitters and devices that satisfy the required Commission International de L'Eclairge (CIE) coordinates (x, y) = (0.14, 0.08), defined by the National Television System Committee (NTSC), or (0.15, 0.06), defined by High-Definition Television (HDTV) ITU-R BT.709. Generally, unbalanced carrier injection and transportation in OLEDs increase driving voltages and decrease device efficiency. Donor–acceptor (DA) type organic light-emitting compounds tend to improve charge balancing in OLEDs, and using DA type compounds would enhance electroluminescence efficiency.[2] On the other hand, DA molecular systems tend to extend π-conjugation and create an intramolecular charge-transfer (ICT) state, which induces a large bathochromic shift and impairs the color purity of emission, showing a broad full-width at half-maximum (FWHM). Accordingly, it is clear that limited π-conjugation and functionalization are prerequisites for deep-blue emission. Thus, following are the major challenges in designing DA type deep-blue-light-emitting compounds: 1) reducing the π-conjugation of both donor and acceptor units so as not to extend the π-conjugation length, 2) introducing a weak electron-donating and accepting nature to prevent a bathochromic shift of emission, and 3) achieving appropriate energy levels for balanced electron and hole injection.

In the past decade, numerous DA type blue-emitting fluorescent compounds have been developed for blue OLED applications.[3,4] Lin et al. recently reported a carbazole-dimesitylborane DA type fluorophore with deep-blue CIE coordinates of (0.15, 0.07) (FWHM: 60 nm), but a maximum current efficiency (CE) and external quantum efficiency (EQE) of only 1.6 cd A^{-1} and 2.4%, respectively.[3a] Li et al. achieved a maximum CE value of 5.7 cd A^{-1} and EQE of 5.0% for a twisting DA type triphenylamine-imidazole molecule applied to non-doped blue electroluminescent devices, but insufficient deep-blue emission was observed, with CIE coordinates of (0.15, 0.11) (FWHM: no data).[3b] Zhang et al. and Yu et al. reported efficient deep-blue-emitting materials with a CE of 2.6 cd A^{-1} and an EQE of 3.1% (CIE coordinates: 0.15, 0.09; FWHM: 71 nm) and with a

J.-Y. Hu, Prof. Y.-J. Pu, F. Satoh, S. Kawata, Prof. H. Katagiri, Prof. H. Sasabe, Prof. J. Kido
Department of Organic Device Engineering
Research Center for Organic Electronics
Yamagata University, 4–3–16, Johnan, Yonezawa, 992–8510, Japan
E-mail: pu@yz.yamagata-u.ac.jp; kid@yz.yamagata-u.ac.jp

DOI: 10.1002/adfm.201302907

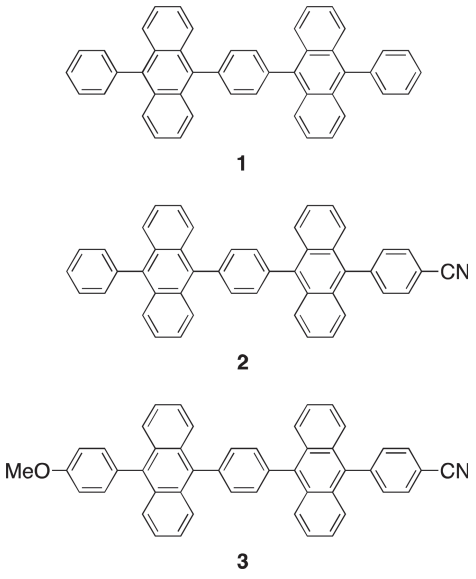

Figure 1. Chemical structures of deep-blue-emitting anthracene compounds **BD1**, **BD2**, and **BD3**.

CE of 1.2 cd A^{-1} and an EQE of 2.0% (CIE coordinates: 0.15, 0.07; FWHM: no data), respectively.[3c,d] Adachi et al. reported deep-blue OLEDs with CIE coordinates of (0.15, 0.07) (FWHM: no data), a high EQE value of 9.9% at low current density, and 2.3% at 100 cd/m^2,[4a] on the basis of thermally activated delayed fluorescence.[4] However, in this device, a large roll-off in efficiency will have to be solved by the optimization of charge balance. On the other hand, 9,10-diphenylanthracene derivatives produce high photoluminescence (PL), exhibit high electrochemical stability to oxidation and reduction, and demonstrate appropriate energy levels for the injection of holes and electrons from a hole-transporting layer and an electron-transporting layer, respectively.[5] Their excited triplet energy is approximately 1.6 eV and able to reproduce a high singlet-excited state, corresponding to the energy of blue emission, by a triplet–triplet annihilation (TTA) process.[6] These properties are advantageous for achieving good charge balance, device efficiency, and stability. Therefore, diphenylanthracene derivatives have been widely used as hosts or emitting dopants in blue OLED applications.[7] However, there are only a few reports on NTSC standard deep-blue OLEDs, based on diphenylanthracene derivatives, and for these, the CE and EQE values need to be improved.[8] To date, no reports of highly efficient HDTV standard deep-blue OLEDs are available, except a few recent reports.[3c,e,9] In this study, we synthesized an DA type blue-emitting compound, 1-(10-(4-methoxyphenyl)anthracen-9-yl)-4-(10-(4-cyanophenyl)anthracen-9-yl)benzene (**BD3**). For comparison, a non DA type compound, 1,4-bis(10-phenylanthracene-9-yl)benzene (**BD1**) and a weak DA type compound, 1-(10-phenylanthracen-9-yl)-4-(10-(4-cyanophenyl)anthracen-9-yl)-benzene (**BD2**), (**Figure 1**) were also synthesized. These molecules were designed on the basis of the following concepts: π-conjugation between the donor unit of 9-(4-methoxyphenyl)anthracene and acceptor unit of 9-cyanophenylanthracene is interrupted by the twisted central benzene core; the non-extended conjugation of the diphenylanthracene unit produces deep-blue emission; and the donor and acceptor units trap holes and electrons, resulting in good charge balance in the corresponding OLEDs. With these blue-emitting compounds as emitters or dopants, our BD3 devices achieved the following: 1) The non-doped blue **BD3** device exhibited a maximum EQE value of 4.2% with a slight roll-off, indicating good charge balance in this device, which was due to the DA type molecular design. 2) The device incorporating a **BD3**-doped CBP host showed a deep-blue emission and maximum CE and EQE of 6.1 cd A^{-1} and 12%, respectively, with CIE coordinates of (0.15, 0.06) (FWHM: 45 nm): features which represent the purest blue fluorescent OLED, emitting nearest to the HDTV standard blue. The **BD3**-based HDTV standard deep-blue OLED showed the best performance with regard to electroluminescence (EL) efficiency and emission color purity among the previously reported devices consisting of small-molecule fluorescent deep-blue OLEDs with CIE coordinate (*y*) of <0.10 (summarized in Table S1).[3a,d,e,4a,7a,b,e–g,i,k,l,8–10]

2. Results and Discussion

The synthetic routes for these anthracene-based blue-emitting compounds are shown in **Scheme 1**. The important intermediates, 9-arylanthracenes (**3a–c**), 9-bromo-10-arylanthracenes (**4a–c**), 10-(4-chlorophenyl)-9-arylanthracenes (**5a–b**), and 4,4,5,5-tetramethyl-2-(4-(10-phenylanthracen-9-yl)-phenyl-1,3,2-dioxaborolanes (**6a–b**), were synthesized according to previously reported methods.[11] The final compounds (**BD1–3**) were then successfully prepared in high yields by Suzuki cross-coupling reactions of 9-bromo-10-arylanthracenes (**4a** and **4c**) and the boronic esters of diarylanthracenes (**6a** and **6b**). These target compounds were fully characterized by ^{1}H NMR, mass spectroscopy, and elemental analysis. By thermogravimetric analysis (TGA), all molecules exhibited high thermal stability showing 5% weight loss decomposition temperatures of 429, 440, and

Table 1. Physical data of the compounds.

	T_m/T_d[a] [°C]	λ_{abs}[b] [nm]	λ_{abs}[c] [nm]	λ_{em}[b] [nm]	λ_{em}[c] [nm]	PLQE[d] [%]	HOMO[e] [eV]	LUMO[e] [eV]	E_g[f] [eV]
BD1	408/429	358/377/398	403	412/419/420	443	77 (14)	−5.95 (−5.45)	−3.02 (−2.07)	2.93
BD2	376/440	358/377/398	404	421/428/434	447	81 (23)	−6.01 (−5.56)	−3.03 (−2.32)	2.98
BD3	415/450	358/378/398	405	422/429/447	452	82 (33)	−6.01 (−5.52)	−3.03 (−2.31)	2.98

[a] Melting point/decomposition temperature (5% weight loss); [b] Toluene solutions (room temperature); [c] Neat thin films; [d] CBP host doped with 3 wt% of compound. Values in parentheses are obtained from neat films; [e] Values in parentheses represent DFT calculations; [f] Energy gap is estimated from the intersection of the absorptions in thin films.

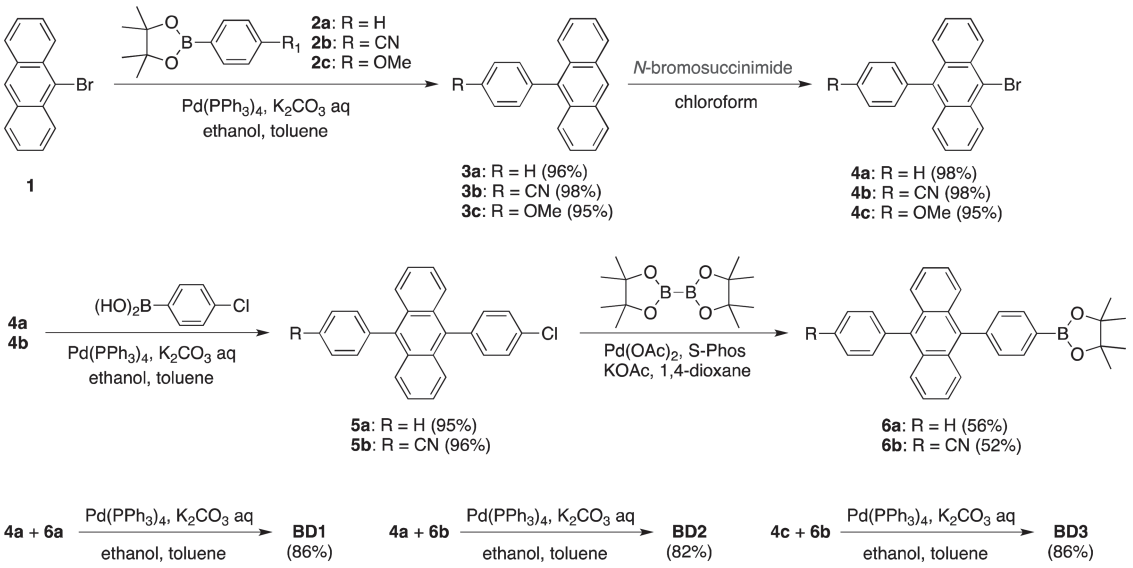

Scheme 1. Synthetic route for compounds **BD1**, **BD2**, and **BD3**.

450 °C for **BD1**, **BD2**, and **BD3**, respectively. By differential scanning calorimetry (DSC), we observed melting temperatures (T_m) of 408 °C, 376 °C, and 415 °C for **BD1**, **BD2**, and **BD3**, respectively; note that no glass-transition temperatures (T_g) were observed. All data are presented in **Table 1**. The molecular structures of **BD1**, **BD2**, and **BD3** were characterized by single-crystal X-ray diffraction analysis, and the key crystallographic data are summarized in Table S2.[12] As shown in **Figures 2** and S1, the two anthracene rings are twisted from the central benzene core by dihedral angles 81° and 82° in **BD1**, 77° and 74° in **BD2**, and 87° and 67° in **BD3**. These twisted conformations of the two anthracene units in the compounds effectively prevent the uninterrupted π-conjugation of the whole molecule and bathochromic shift of emission and separate the highest occupied molecular orbital (HOMO) (based on the donor unit) and the lowest unoccupied molecular orbital (LUMO) (based on the acceptor unit).

Density functional theory (DFT) calculations (B3LYP) were performed for **BD1**, **BD2**, and **BD3** with the 6–311+G(d,p)//6–31G(d) basis set by using the Gaussian 09 program.[13] The calculated dipole moments were 0.00 for **BD1** (derived from its nonpolar symmetrical structure), and 6.79 for **BD3**, higher than the value of 5.86 for **BD2** (derived from the stronger electron-donating property of the methoxyphenyl group of **BD3**) compared with that for the unsubstituted phenyl group of **BD2**. The spatial distribution of the molecular orbitals and their energy levels are shown in **Figure 3** and in Figures S2 and S3, respectively. For nonpolar and symmetrical **BD1**, the molecular orbitals of the two anthracene units are independent of each other, and each of the HOMO and LUMO orbitals is energetically degenerate, supporting the speculation that the orthogonally twisted central phenyl group interrupts π-conjugation. On the other hand, in DA type **BD2** and **BD3**, the HOMO is located on the anthracene unit with the electron-rich methoxyphenyl group or unsubstituted phenyl group, and the LUMO is located on the anthracene unit with the electron-withdrawing cyanophenyl group. The lack of overlap between the HOMO and LUMO of **BD2** and **BD3** usually indicates a small energy gap between the exited singlet state and triplet state. However, time-dependent (TD) DFT calculations showed two degenerate lowest triplet levels (T_1 and T_2) of 1.7 eV, which is much lower than the value of the S_1 level (2.9 eV) (**Table 2** and Figure S4). These lowest triplet states are ascribed to the transition from HOMO-1 to LUMO and from HOMO to LUMO+1, both located

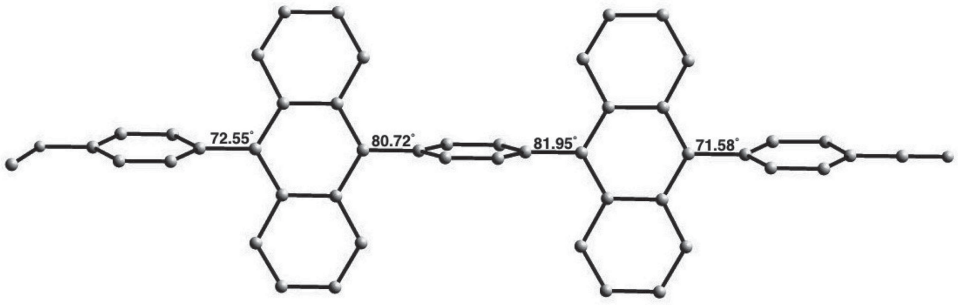

Figure 2. Molecular structure of **BD3** obtained by single-crystal X-ray analysis, depicting dihedral angles of adjacent aromatic rings.

Table 2. Calculated energy levels, oscillator strengths (f), and orbital transition analyses for BD3.

Excited state	E_g [eV]	E_g [nm]	f	Transition (D: donor unit, A: acceptor unit)			Coefficient
S_1	2.8811	430.34	0.0008	D: HOMO	–>	A: LUMO	0.70647
S_2	3.0267	409.64	0.4113	A: HOMO-1	–>	A: LUMO	0.55963
				D: HOMO	–>	D: LUMO+1	–0.41919
S_3	3.0822	402.25	0.0063	A: HOMO-1	–>	A: LUMO	0.41531
				D: HOMO	–>	D: LUMO+1	0.56080
S_4	3.2766	378.39	0.0002	A: HOMO-1	–>	A: LUMO+2	0.69889
S_5	3.3045	375.20	0.0000	A: HOMO-1	–>	D: LUMO+1	0.70572
S_6	3.4575	358.59	0.0000	D: HOMO	–>	A: LUMO+2	0.70563
S_7	3.6281	341.73	0.0002	D: HOMO-2	–>	D: LUMO+1	0.70307
T_1	1.7290	717.10	0.0000	A: HOMO-1	–>	A: LUMO	0.69452
				A: HOMO-1	<–	A: LUMO	0.13089
T_2	1.7324	715.67	0.0000	D: HOMO	–>	D: LUMO+1	0.69724
				D: HOMO	<–	D: LUMO+1	0.13193
T_3	2.8809	430.36	0.0000	D: HOMO	–>	A: LUMO	0.70587
T_4	3.1984	387.65	0.0000	HOMO-9	–>	A: LUMO+2	0.27324
				A: HOMO-1	–>	A: LUMO+2	0.63071
T_5	3.2346	383.30	0.0000	HOMO-10	–>	A: LUMO	–0.26072
				HOMO-8	–>	A: LUMO	0.28073
				HOMO-7	–>	A: LUMO	0.3035
				A: HOMO-1	–>	LUMO+3	–0.16313
				A: HOMO-1	–>	LUMO+4	0.18503
				A: HOMO-1	–>	LUMO+8	0.19637
				A: HOMO-1	–>	LUMO+9	0.15593
				A: HOMO-1	–>	LUMO+10	0.25751
T_6	3.2394	382.74	0.0000	HOMO-10	–>	D: LUMO+1	0.13403
				HOMO-8	–>	D: LUMO+1	0.25212
				HOMO-5	–>	D: LUMO+1	0.41053
				HOMO-4	–>	D: LUMO+1	0.12624
				D: HOMO	–>	LUMO+4	0.10272
				D: HOMO	–>	LUMO+5	–0.11092
				D: HOMO	–>	LUMO+7	–0.22408
				D: HOMO	–>	LUMO+13	0.32355
T_7	3.3038	375.27	0.0000	A: HOMO-1	–>	D: LUMO+1	0.70598

on the same anthracene unit. The transitions between spatially non-overlapped HOMO and LUMO orbitals are ascribed to S_1 and T_3, and their energy difference is zero. HOMO-1 and LUMO+1 also do not overlap, and the transitions between them are ascribed to S_5 and T_7; their energy difference is also zero. These zero gaps between the exited singlet ($S_n \geq _1$) and triplet ($T_m \geq _3$) state may offer some advantage with respect to increasing the radiative singlet-state population from the non-radiative high triplet state, generated by the TTA of the T_1 and T_2 states.

UV/vis absorption and PL spectra of **BD**, **BD2**, and **BD3** in toluene solution and as neat films were measured, and the data are summarized in Table 1. All compounds showed three absorption peaks in the toluene solution at 358, 377, and 399 nm, ascribed to the vibrational structure of the anthracene unit, and strong blue photoluminescence as solutions and films. The PL spectra in hexane, toluene, and 1,2-dichloromethane solution showed almost identical blue emissions, and the bathochromic shift of the emission peak acquired in polar 1,2-dichloromethane solution compared with that acquired in nonpolar hexane solution was only 9 nm (**Figures 4**a and S5). These emissions, which were less dependent on solvent polarity, indicated that the electron-donating property of the donor unit and the electron-accepting

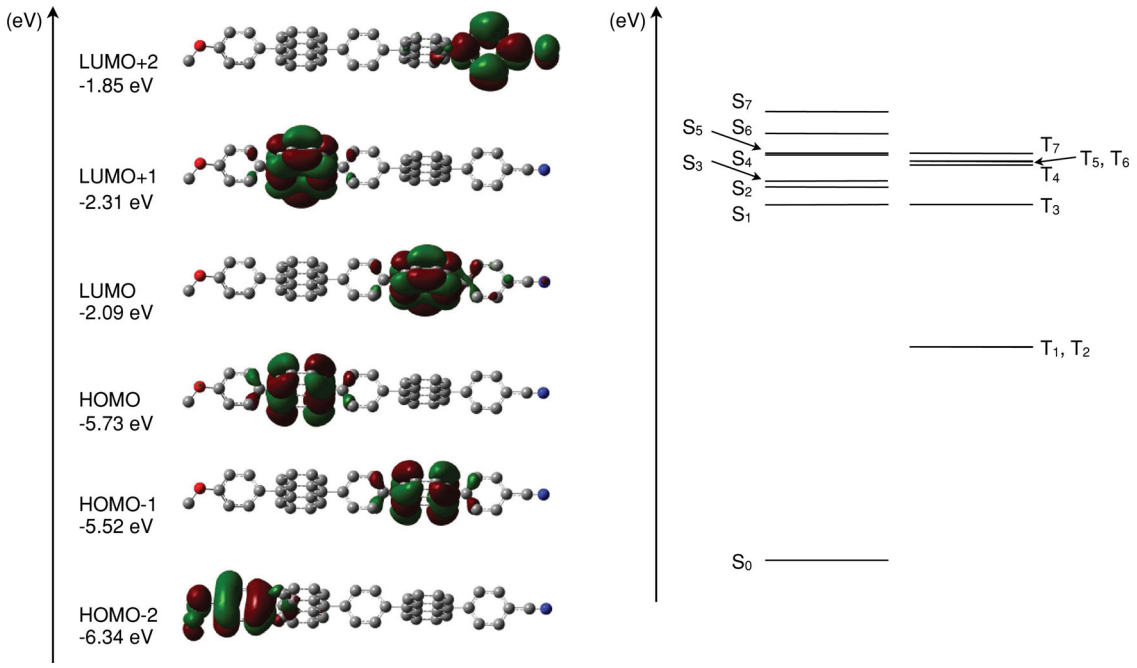

Figure 3. Calculated energy levels, molecular orbitals, and excited state of **BD3**.

property of the acceptor unit of the compounds are sufficiently weak such that they do not produce an ICT state, which results in an undesired bathochromic shift of the emission on photoexcitation. This result indicates that the deep-blue-emitting feature of biarylanthracene **BD1** can be maintained after modification to **BD2** and **BD3**, which incorporate weak DA type features. In the films, the more polar compounds with the order of the dipole moment showed a longer emission tail in the PL spectrum, probably ascribable to excimer emission because of stronger intermolecular interactions (Figure 4b). The PL quantum efficiencies were measured by an integrating sphere system. In the CBP host with 3 wt% doping concentration, **BD3** showed 82% PLQE, comparable to the values for **BD2** and **BD1** (Table 1). This high PLQE of **BD3** demonstrated that the introduction of the electron-donating and -withdrawing groups on bianthracene **BD1** did not degrade the high PL property of **BD1**. The HOMO energy levels were estimated to be 5.95, 6.01, and 6.01 eV for **BD1**, **BD2**, and **BD3**, respectively, from the ionization potential obtained by photoelectron yield spectroscopy. The LUMO energy levels were estimated to be 3.02, 3.03, and 3.03 eV for **BD1**, **BD2**, and **BD3**, respectively, from the difference between the HOMO levels and the optical energy gaps (2.93, 2.98, and 2.98 eV for **BD1**, **BD2**, and **BD3**, respectively) determined from the UV absorption edges (Table 1).

Initially, we investigated the performance of non-doped blue-emitting devices **1**–**3**. 1,1′-Bis(di-4-tolyl-aminophenyl) cyclohexane (TAPC) was used as a hole-transport material, and 3,5,3″,5″-tetra-3-pyridyl-1,1′;3′,1″-terphenyl (B3PyPB) was used as the electron-transport material.[14] The device structures were composed of ITO/TAPC (40 nm)/**BD** compound (20 nm)/B3PyPB (40 nm)/LiF (1 nm)/Al (80 nm), where the **BD** compound for devices **1**, **2**, and **3** was **BD1**, **BD2**, and **BD3**, respectively. The device characteristics are shown in **Table 3** and Figure S6. All devices (**1**–**3**) exhibited blue electroluminescence with CIE coordinates of (0.17, 0.13) for device **1**, (0.18, 0.20) for device **2**, and (0.24, 0.17) for device **3**, consistent with the PL spectra of the compounds. Device **1** with **BD1** as the emitter showed the highest EQE value (5.6%), although the PLQE of

Table 3. Electroluminescent data of the devices.

Device	Compound	λ_{EL}[a] [nm]	FWHM[a] [nm]	CIE (x, y)[a]	V_{on}[b] [V]	$CE_{max/100/1000}$[c] [cd/A]	Power efficiency $(PE)_{max/100/1000}$[c] [lm/W]	$EQE_{max/100/1000}$[c] [%]
1	**BD1**	432	52	0.17, 0.13	3.9	6.7/6.1/4.7	6.2/4.9/2.9	5.6/5.0/4.5
2	**BD2**	443	54	0.18, 0.20	3.8	4.8/3.8/3.8	5.0/3.1/2.4	3.0/2.4/2.7
3	**BD3**	445	55	0.24, 0.17	3.9	8.2/6.2/5.8	8.6/5.0/3.7	4.2/3.2/3.1
A	**BD1**	424	44	0.16, 0.05	3.4	3.9/1.8/1.5	3.8/1.2/0.66	8.9/4.3/3.7
B	**BD2**	430	47	0.15, 0.06	3.5	4.9/2.7/1.9	4.8/1.6/0.81	9.5/5.2/4.0
C	**BD3**	432	45	0.15, 0.06	3.7	6.1/2.6/2.0	5.6/1.5/0.85	12/5.3/4.2

[a]At 100 cd m^{-2}; [b]At 1 cd m^{-2}; [c] Maximum at 100 cd m^{-2}/at 1000 cd m^{-2}.

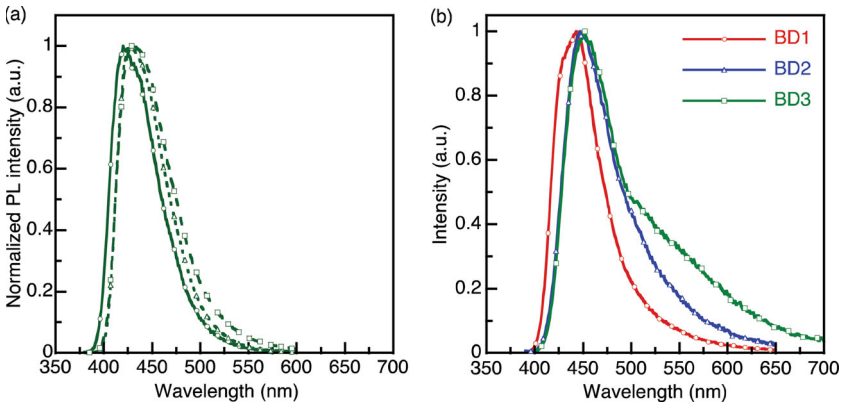

Figure 4. (a) PL spectra of **BD3** in hexane (solid line), toluene (dotted line), and 1,2-dichloromethane (dashed line). (b) PL spectra of **BD1**, **BD2**, and **BD3** neat films.

the neat film was only 14%. If we use the following simple equation to evaluate the EQE value of device **1**: [EQE] = [charge balance]·[PLQE]·[singlet exciton ratio]·[outcoupling efficiency], the charge balance and singlet exciton ratio should be 100%, and the outcoupling efficiency should be 40%. These are the possible maxima for each parameter; however, we must be very careful to use the optically obtained PLQE (14%) in this case, and thus further study is needed. Note that the EQE roll-off for devices **2** and **3** is smaller than that for device **1**, indicating good charge balance resulting from the DA type molecular structure. The performance values for devices **1**–**3** are comparable with the highest value reported for certain non-doped blue OLEDs with a CIE coordinate (y) of ~0.15.[10b,15]

To further investigate the potential application of these blue-emitting compounds, we fabricated doped OLED devices with the structure ITO/TAPC (40 nm)/emitting layer (20 nm)/B3PyPB (40 nm)/LiF/Al, where **BD1** (device **A**), **BD2** (device **B**), and **BD3** (device **C**) were used as the emitting dopant in the CBP host. As shown in **Figure 5**a, all the resulting EL spectra showed an emission peak around 424–432 nm with a narrow FWHM of 44, 47, and 45 nm for device **A**, **B**, and **C**, respectively, which corresponded well with the PL spectra in solution (Figure S7). More specifically, all these EL spectra exhibited saturated blue emission with CIE coordinates of (0.16, 0.05), (0.15, 0.06), and (0.15, 0.06) for **BD1**-, **BD2**-, and **BD3**-based devices, respectively. In particular, the **BD2**- and **BD3**-based devices exhibited an emission nearest to the HDTV standard blue color (inset of Figure 5a). The performance of devices **A**–**C** is summarized in Table 3. All of these dopant–emitter-based devices showed excellent EL efficiencies in the current density range of 1–100 mA cm^{-2}. More remarkably, when **BD3** was used as the dopant emitter, the maximum efficiency was 6.1 cd A^{-1} (5.6 lm W^{-1}) at 0.002 mA cm^{-2}, and the EQE value was 12%. This is the best CE value reported to date for deep-blue OLEDs (CIE coordinate (y) of 0.06). Although there is a roll-off in EL efficiency at high current density in the **BD3**-based device, a 4.0% EQE value was obtained even at 1800 cd m^{-2} (100 mA cm^{-2}). Overall, device **C** showed the best performance with respect to EL efficiency and emission color purity among the devices consisting of small-molecule fluorescent deep-blue OLEDs with a CIE coordinate (y) of <0.10 (summarized in Table S1).

The high performance of the **BD3**-doped device with the CBP host may be attributed to several possible factors: 1) Choosing an appropriate host and optimizing the dopant concentration are important steps toward high device performance. As shown in Figure S9, the overlap between the absorption spectrum of **BD3** and the PL spectrum of CBP was significant, allowing efficient host-to-guest Förster energy transfer, and consequently, highly improved efficiency. The PL spectra of the **BD3**-doped CBP film showed that the emission of CBP completely disappeared with a small amount of **BD3** (1–6 wt% concentration), indicating complete energy transfer. 2) Using the DA type light-emitting dopant is an important factor for achieving high device performance. In this study, in comparison with nonpolar **BD1**, DA type **BD2** and **BD3** have a balanced energy level between the donor and acceptor, which could contribute to a good balance between electron and hole currents in the OLED devices. An energy diagram is shown in Figure S10. The HOMO energy level of the BD dopant is shallower than that of the CBP host, while the LUMO level is deeper. This energy level alignment of

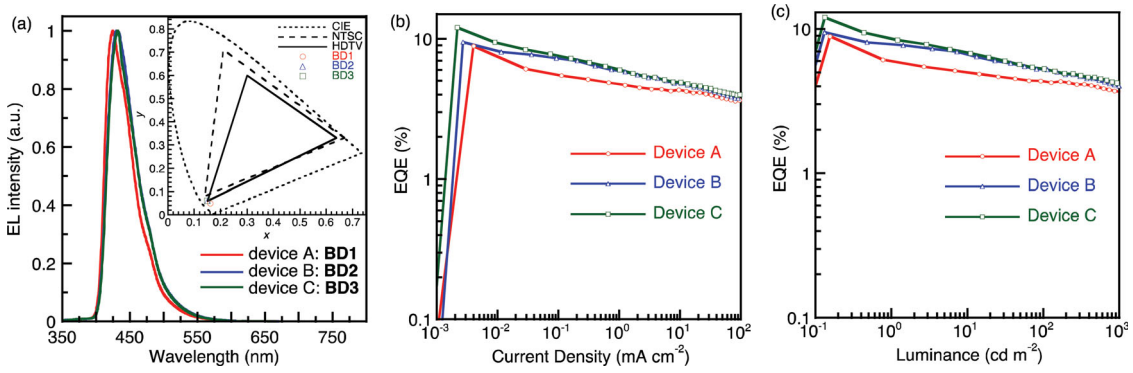

Figure 5. (a) EL spectra of **BD** (A), **BD2** (B), and **BD3** (C) doped in a CBP layer. Inset: The CIE coordinates of the EL spectra of devices A–C. (b) The EQE–current density plots of the OLEDs based on compounds **BD**, **BD2**, and **BD3**.

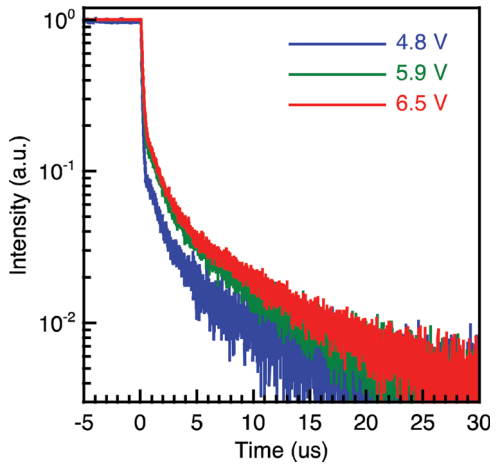

Figure 6. Time-resolved electroluminescence response of the **BD3**-doped CBP-based device C under various excitation pulse voltages.

the emitting dopant and host may contribute to the direct trapping of holes and electrons on the dopant, resulting in the good charge balance and high efficiency. 3) TTA may have played an important role in increasing the EQE value of the device by up to 10%. In this study, the PLQE of 3 wt% **BD3** in the CBP film was measured to be 83%. Therefore, the theoretical upper limit for EQE would be in the range 4.2%–6.2%, depending on the outcoupling efficiency. Thus, we proposed that the measured EQE value, which was much higher than the theoretically obtained values, could be mainly caused by increased singlet excitons resulting from the TTA process.[6,16] The transient electroluminescence responses of the **BD3**-doped device C were measured (**Figure 6**). In device C, the electroluminescence rapidly decreased on the order of sub-microseconds at the end of the excitation pulse owing to the short fluorescence lifetime of the emitting molecules. After the first rapid component, a delayed electroluminescence component on the order of several tens of microseconds was observed. Just after applying a forward-pulse voltage, the –5 V of the reverse-pulse voltage was applied to eliminate any trapped charges, so that the observed delayed components are not due to the recombination of trapped charges, but by emission from the TTA process.

3. Conclusion

Three types of blue-light-emitting benzene-cored phenylanthracene-functionalized molecules have been designed and synthesized by a convergent approach using stepwise palladium-catalyzed Suzuki cross-coupling reactions. All compounds exhibited high thermal and amorphous morphological stabilities and deep-blue fluorescence. The OLED devices based on these molecules as host or dopant emitters exhibited blue emission and high efficiency. In particular, with the DA type molecule **BD3** as a dopant, the device exhibited an efficiency level of up to 6.1 cd A^{-1} at 2 mA cm^{-2}, an EQE value of up to 10%, and CIE coordinates of (0.15, 0.06) with a narrow FWHM of 45 nm, which is close to the CIE of the HDTV standard blue. These results provide a molecular design concept leading to highly efficient deep-blue-emitting molecules for OLED applications.

Supporting Information

Supporting Information is available from the Wiley Online Library or from the author.

Acknowledgements

This study was supported by an Industrial Technology Research Grant for Young Researchers from the New Energy and Industrial Technology Development Organization (NEDO). We would like to thank the partial support by Japan Regional Innovation Strategy Program by the Excellence (J-RISE) (Creating international research hub for advanced organic electronics) of Japan Science and Technology Agency (JST).

Received: August 19, 2013
Revised: September 12, 2013
Published online: December 4, 2013

[1] a) N. C. Giebink, B. W. D'Andrade, M. S. Weaver, P. B. Mackenzie, J. J. Brown, M. E. Thompson, S. R. Forrest, *J. Appl. Phys.* **2008**, *103*, 44509; b) I. R. de Moraes, S. Scholz, B. Lussem, K. Leo, *Org. Electron.* **2011**, *12*, 341.

[2] a) Y. Shirota, M. Kinoshita, T. Noda, K. Okumoto, T. Ohara, *J. Am. Chem. Soc.* **2000**, *122*, 11021; b) H. Doi, M. Kinoshita, K. Okumoto, Y. Shirota, *Chem. Mater.* **2003**, *15*, 1080; c) T. H. Huang, J. T. Lin, L. Y. Chen, Y. T. Lin, C. C. Wu, *Adv. Mater.* **2006**, *18*, 602; d) A. P. Kulkarni, X. X. Kong, S. A. Jenekhe, *Adv. Funct. Mater.* **2006**, *16*, 1057.

[3] a) S. L. Lin, L. H. Chan, R. H. Lee, M. Y. Yen, W. J. Kuo, C. T. Chen, R. J. Jeng, *Adv. Mater.* **2008**, *20*, 3947; b) W. J. Li, D. D. Liu, F. Z. Shen, D. G. Ma, Z. M. Wang, T. Feng, Y. X. Xu, B. Yang, Y. G. Ma, *Adv. Funct. Mater.* **2012**, *22*, 2797; c) Y. Zhang, S. L. Lai, Q. X. Tong, M. F. Lo, T. W. Ng, M. Y. Chan, Z. C. Wen, J. He, K. S. Jeff, X. L. Tang, W. M. Liu, C. C. Ko, P. F. Wang, C. S. Lee, *Chem. Mater.* **2012**, *24*, 61; d) D. H. Yu, F. C. Zhao, Z. Zhang, C. M. Han, H. Xu, J. Li, D. G. Ma, P. F. Yan, *Chem. Commun.* **2012**, *48*, 6157; e) J. Ye, Z. Chen, M.-K. Fung, C. Zheng, X. Ou, X. Zhang, Y. Yuan, C.-S. Lee, *Chem. Mater.* **2013**, *25*, 2630.

[4] a) Q. S. Zhang, J. Li, K. Shizu, S. P. Huang, S. Hirata, H. Miyazaki, C. Adachi, *J. Am. Chem. Soc.* **2012**, *134*, 14706; b) G. Méhes, H. Nomura, Q. S. Zhang, T. Nakagawa, C. Adachi, *Angew. Chem. Int. Ed.* **2012**, *51*, 11311; c) H. Uoyama, K. Goushi, K. Shizu, H. Nomura, C. Adachi, *Nature* **2012**, *492*, 234.

[5] K. Okumoto, H. Kanno, Y. Hamada, H. Takahashi, K. Shibata, *J. Appl. Phys.* **2006**, *100*.

[6] a) D. Y. Kondakov, *J. Appl. Phys.* **2007**, *102*, 114504; b) D. Y. Kondakov, T. D. Pawlik, T. K. Hatwar, J. P. Spindler, *J. Appl. Phys.* **2009**, *106*, 124510.

[7] a) Y. H. Kim, H. C. Jeong, S. H. Kim, K. Y. Yang, S. K. Kwon, *Adv. Funct. Mater.* **2005**, *15*, 1799; b) M. H. Ho, Y. S. Wu, S. W. Wen, M. T. Lee, T. M. Chen, C. H. Chen, K. C. Kwok, S. K. So, K. T. Yeung, Y. K. Cheng, Z. Q. Gao, *Appl. Phys. Lett.* **2006**, *89*, 252903; c) Z. Q. Gao, B. X. Mi, C. H. Chen, K. W. Cheah, Y. K. Cheng, W. S. Wen, *Appl. Phys. Lett.* **2007**, *90*, 123506; d) Y. Y. Lyu, J. Kwak, O. Kwon, S. H. Lee, D. Kim, C. Lee, K. Char, *Adv. Mater.* **2008**, *20*, 2720; e) Y. I. Park, J. H. Son, J. S. Kang, S. K. Kim, J. H. Lee, J. W. Park, *Chem. Commun.* **2008**, 2143; f) S. K. Kim, B. Yang, Y. Ma, J. H. Lee, J. W. Park, *J. Mater. Chem.* **2008**, *18*, 3376; g) C. H. Chien, C. K. Chen, F. M. Hsu, C. F. Shu, P. T. Chou, C. H. Lai, *Adv. Funct.*

Mater. **2009**, *19*, 560; h) M. R. Zhu, Q. A. Wang, Y. Gu, X. S. Cao, C. Zhong, D. G. Ma, J. G. Qin, C. L. Yang, *J. Mater. Chem.* **2011**, *21*, 6409; i) T. Zhang, D. Liu, Q. Wang, R. J. Wang, H. C. Ren, J. Y. Li, *J. Mater. Chem.* **2011**, *21*, 12969; j) K. H. Lee, J. K. Park, J. H. Seo, S. W. Park, Y. S. Kim, Y. K. Kim, S. S. Yoon, *J. Mater. Chem.* **2011**, *21*, 13640; k) I. Cho, S. H. Kim, J. H. Kim, S. Park, S. Y. Park, *J. Mater. Chem.* **2012**, *22*, 123; l) S. Tang, W. J. Li, F. Z. Shen, D. D. Liu, B. Yang, Y. G. Ma, *J. Mater. Chem.* **2012**, *22*, 4401.

[8] a) Y. H. Kim, D. C. Shin, S. H. Kim, C. H. Ko, H. S. Yu, Y. S. Chae, S. K. Kwon, *Adv. Mater.* **2001**, *13*, 1690; b) J. H. Jou, Y. P. Lin, M. F. Hsu, M. H. Wu, P. Lu, *Appl. Phys. Lett.* **2008**, *92*, 193314.

[9] H. T. Shih, C. H. Lin, H. H. Shih, C. H. Cheng, *Adv. Mater.* **2002**, *14*, 1409.

[10] a) C. C. Wu, Y. T. Lin, K. T. Wong, R. T. Chen, Y. Y. Chien, *Adv. Mater.* **2004**, *16*, 61; b) C. J. Tonzola, A. P. Kulkarni, A. P. Gifford, W. Kaminsky, S. A. Jenekhe, *Adv. Funct. Mater.* **2007**, *17*, 863; c) Z. Q. Gao, Z. H. Li, P. F. Xia, M. S. Wong, K. W. Cheah, C. H. Chen, *Adv. Funct. Mater.* **2007**, *17*, 3194; d) Z. Zhang, H. Tang, H. F. Wang, X. Liang, J. Liu, Y. Qiu, G. Q. Shi, *Thin Solid Films* **2007**, *515*, 3893; e) J. Luo, Y. Zhou, Z. Q. Niu, Q. F. Zhou, Y. G. Ma, J. Pei, *J. Am. Chem. Soc.* **2007**, *129*, 11314; f) J. N. Moorthy, P. Venkatakrishnan, D. F. Huang, T. J. Chow, *Chem. Commun.* **2008**, 2146; g) B. D. Ding, W. Q. Zhu, X. Y. Jiang, Z. L. Zhang, *Curr. Appl. Phys.* **2008**, *8*, 573; h) N. Matsumoto, T. Miyazaki, M. Nishiyama, C. Adachi, *J. Phys. Chem. C* **2009**, *113*, 6261; i) Y. Y. Li, H. B. Wu, J. H. Zou, L. Ying, W. Yang, Y. Cao, *Org. Electron.* **2009**, *10*, 901; j) Z. Q. Jiang, Z. Y. Liu, C. L. Yang, C. Zhong, J. G. Qin, G. Yu, Y. Q. Liu, *Adv. Funct. Mater.* **2009**, *19*, 3987; k) A. L. Fisher, K. E. Linton, K. T. Kamtekar, C. Pearson, M. R. Bryce, M. C. Petty, *Chem. Mater.* **2011**, *23*, 1640; l) X. Xing, L. P. Zhang, R. Liu, S. Y. Li, B. Qu, Z. J. Chen, W. F. Sun, L. X. Xiao, Q. H. Gong, *ACS Appl. Mater. Interfaces* **2012**, *4*, 2877; m) X. Xing, L. X. Xiao, L. L. Zheng, S. Y. Hu, Z. J. Chen, B. Qu, Q. H. Gong, *J. Mater. Chem.* **2012**, *22*, 15136; n) K. Wang, F. Zhao, C. Wang, S. Chen, D. Chen, H. Zhang, Y. Liu, D. Ma, Y. Wang, *Adv. Funct. Mater.* **2013**, *23*, 2672.

[11] J.-Y. Hu, Y.-J. Pu, Y. Yamashita, F. Satoh, S. Kawata, H. Katagiri, H. Sasabe, J. Kido, *J. Mater. Chem. C* **2013**, *1*, 3871.

[12] CCDC No. 949384 for BD1, No. 949385 for BD2, and No. 949386 for BD3.

[13] M. J. Frisch, G. W. Trucks, H. B. Schlegel, G. E. Scuseria, M. A. Robb, J. R. Cheeseman, G. Scalmani, V. Barone, B. Mennucci, G. A. Petersson, H. Nakatsuji, M. Caricato, X. Li, H. P. Hratchian, A. F. Izmaylov, J. Bloino, G. Zheng, J. L. Sonnenberg, M. Hada, M. Ehara, K. Toyota, R. Fukuda, J. Hasegawa, M. Ishida, T. Nakajima, Y. Honda, O. Kitao, H. Nakai, T. Vreven, J. J. A. Montgomery, J. E. Peralta, F. Ogliaro, M. Bearpark, J. J. Heyd, E. Brothers, K. N. Kudin, V. N. Staroverov, R. Kobayashi, J. Normand, K. Raghavachari, A. Rendell, J. C. Burant, S. S. Iyengar, J. Tomasi, M. Cossi, N. Rega, J. M. Millam, M. Klene, J. E. Knox, J. B. Cross, V. Bakken, C. Adamo, J. Jaramillo, R. Gomperts, R. E. Stratmann, O. Yazyev, A. J. Austin, R. Cammi, C. Pomelli, J. W. Ochterski, R. L. Martin, K. Morokuma, V. G. Zakrzewski, G. A. Voth, P. Salvador, J. J. Dannenberg, S. Dapprich, A. D. Daniels, Ö. Farkas, J. B. Foresman, J. V. Ortiz, J. Cioslowski, D. J. Fox, Revision A.02 ed., Gaussian Inc, Wallingford CT, **2009**.

[14] H. Sasabe, E. Gonmori, T. Chiba, Y. J. Li, D. Tanaka, S. J. Su, T. Takeda, Y. J. Pu, K. I. Nakayama, J. Kido, *Chem. Mater.* **2008**, *20*, 5951.

[15] a) H. C. Li, Y. P. Lin, P. T. Chou, Y. M. Cheng, R. S. Liu, *Adv. Funct. Mater.* **2007**, *17*, 520; b) P. I. Shih, C. Y. Chuang, C. H. Chien, E. W. G. Diau, C. F. Shu, *Adv. Funct. Mater.* **2007**, *17*, 3141; c) Y. L. Liao, C. Y. Lin, K. T. Wong, T. H. Hou, W. Y. Hung, *Org. Lett.* **2007**, *9*, 4511; d) S. B. Jiao, Y. Liao, X. J. Xu, L. P. Wang, G. Yu, L. M. Wang, Z. M. Su, S. H. Ye, Y. Q. Liu, *Adv. Funct. Mater.* **2008**, *18*, 2335; e) S. J. Lee, J. S. Park, K. J. Yoon, Y. I. Kim, S. H. Jin, S. K. Kang, Y. S. Gal, S. Kang, J. Y. Lee, J. W. Kang, S. H. Lee, H. D. Park, J. J. Kim, *Adv. Funct. Mater.* **2008**, *18*, 3922; f) S. L. Tao, Y. C. Zhou, C. S. Lee, X. H. Zhang, S. T. Lee, *Chem. Mater.* **2010**, *22*, 2138; g) S. O. Kim, K. H. Lee, G. Y. Kim, J. N. Seo, Y. K. Kim, S. S. Yoon, *Synth. Met.* **2010**, *160*, 1259; h) K. H. Lee, L. K. Kang, J. Y. Lee, S. Kang, S. O. Jeon, K. S. Yook, J. Y. Lee, S. S. Yoon, *Adv. Funct. Mater.* **2010**, *20*, 1345; i) M. R. Zhu, T. L. Ye, C. G. Li, X. S. Cao, C. Zhong, D. G. Ma, J. G. Qin, C. L. Yang, *J. Phys. Chem. C* **2011**, *115*, 17965; j) C. G. Zhen, Y. F. Dai, W. J. Zeng, Z. Ma, Z. K. Chen, J. Kieffer, *Adv. Funct. Mater.* **2011**, *21*, 699; k) T. S. Qin, W. Wiedemair, S. Nau, R. Trattnig, S. Sax, S. Winkler, A. Vollmer, N. Koch, M. Baumgarten, E. J. W. List, K. Mullen, *J. Am. Chem. Soc.* **2011**, *133*, 1301; l) J. Huang, N. Sun, J. Yang, R. L. Tang, Q. Q. Li, D. G. Ma, J. G. Qin, Z. Li, *J. Mater. Chem.* **2012**, *22*, 12001.

[16] a) C. Ganzorig, M. Fujihira, *Appl. Phys. Lett.* **2002**, *81*, 3137; b) Z. D. Popovic, H. Aziz, *J. Appl. Phys.* **2005**, *98*, 13510; c) Y. C. Luo, H. Aziz, *Adv. Funct. Mater.* **2010**, *20*, 1285.